Journal of Electroceramics, 12, 89–100, 2004

Piezoelectric Microactuator Devices

R. MAEDA, J.J. TSAUR, S.H. LEE & M. ICHIKI
National Institute of Advanced Industrial Science and Technology, 1-2-1 Namiki, Tsukuba 305-8564, Japan

Abstract. MEMS (Microelectromechanical Systems) R&D originated from the successes of microactuator device fabrication by Si semiconductor micromachining technology. Although this technology is suitable for fabricating microstructures, the sensing and actuation capability employed is limited only to electrostatic and capacitive devices, which results in the limited functions of the devices. In particular, high force output with low power dissipation cannot be achieved by electrostatic actuation. The integration of piezoelectric materials for MEMS is thus highly encouraged to realize high force output as well as sensing capability using both piezoelectric and inverse piezoelectric effects. This integration then results in simplification of the microstructures. Promising applications of piezoactuators and the difficulties of integrating exotic piezoelectric materials in conventional micromachining processes are discussed in this paper.

Keywords: ferroelectric thin films, micro actuator, micro pump, scanning mirror, SFM, micro valve

1. Introduction

Ferroelectric thin film is a target of interest in the fabrication of microelectromechanical systems, memory devices, etc. Piezo-MEMS will be developed with such materials as thin films. In spite of the successful commercialization of FRAM applications, MEMS applications are still being developed. Although there are promising properties, there have been rather few successes in the use of such layers as MEMS devices. Problems in such applications are mainly caused by the very small dimensions required of such devices, in contrast to the limitations and tolerances of the currently used microtechnologies. Although the deposition of piezoelectric PZT-layers using different thin-film technologies has reached an advanced state, layers of more than 1 micron in thickness needed for MEMS applications are still difficult to deposit. When dealing with these problems, researchers must take into account that the structure or function of the devices may be affected by technologically caused constraints, like thickness deviation and deformation by residual stress, and they must also seek to optimize materials processing parameters.

Very much attention has been given to integrating ferroelectric thin films in MEMS for various applications, such as pumps, valves, ink-jet printer heads, ultrasonic fluid drives, and micromirrors, with a focus on changing the length because they have good properties capable of use as driving sources and actuators for microsystems [1–5]. The chief reason for this interest is that we can expect larger force output than that available from electrostatic actuators. However, because of the small strain (usually less than 10%) and high stresses (several MPa) in piezoelectric actuators, their use is suitable for applications with large forces but small displacements [6, 7].

This paper introduces promising applications of piezoactuators. These applications are classified by their shape, cantilever, membrane and bulk types.

2. Cantilever Type Actuators

2.1. Micro Scanning Mirrors

Micromirrors derived from microfabrication technology have received a great deal of attention due to their wide applications in optical information systems ranging from barcode readers and laser positioning components to image scanning projection. Additionally, in fiber optical communication systems including DWDM, micromirrors with precisely controlled block-and-pass positioning are used for the shuttering cells in optical switching arrays.

Most micromirror designs consist of one or more cantilevers that support the mirror plate with a hinge/bar connection. Micromachined actuators, derived from electromagnetic, electrostatic, electrothermal or piezoelectric drivers, are integrated with cantilevers to excite bending vibration and twisting rotation of a micromirror with 1D or 2D motion. In recent years, the electrostatically driven mirror has been the mainstream type using electrical comb actuators or a parallel planar electrode scheme. However, high driving voltage of up to a hundred volts is necessary for the large deflection angle requirement. In addition, the electrostatic pull-in on a planar electrode also results in a non-linearity characteristic relative to the tilting angle. In cases of electrothermal-actuated micromirrors, the slow response cannot satisfy the need of wider bandwidth operations. In contrast, the piezoelectric-actuated mirror can provide relatively lower operation voltage, very low power consumption, and better linearity of deflection. The progress of thin film piezoelectric technology made significant contributions toward the reduction of mirror dimensions which resulted in higher resonant frequencies and the improved piezoelectric characteristics for the necessary driving forces.

In 1966, Fowler et al. developed a piezoelectric optical beam scanner using thick lead zirconate titanate (PZT) layers and coated conductive mediums as electrodes [8]. In 1976, Frank et al. reported on a bimorph beam scanner composed of two PZT layers and introduced a pivot design for magnifying angular excursion with one degree of freedom (1D) [9]. To further reduce mirror dimensions and perform motion with two degrees of freedom (2D), in 1991 Goto et al. proposed a silicon micromachined mirror for which a stacked PZT resonator vibrated a torsional silicon spring to perform bending or twisting motions with 2D scanning [10]. With the objective of achieving a large scanning angle and vibration robustness, Ohtsuka et al. developed a four PZT bimorph-cell-actuated optical scanner [11] and Yee et al. proposed a four PZT unimorph-actuated micromirror [11]. Both of them adopted a silicon-based micromirror supported by symmetrically arranged inner and outer frames to perform 2D torsional motion. Regarding PZT materials, since bulk and thick film PZT are not suitable for miniature devices, thin film technology was widely used to prepare the submicron-thick PZT layer between the upper and lower platinum electrodes. In 1999, Schroth and Maeda reported on a sol-gel-deposited PZT film for a 1D and 2D optical scanner [12]. To eliminate the residual strain generated from annealing in the sol-gel process, a bimorph-like double-layered PZT with bi-directional actuation was used for a 2D microscanner as illustrated in Fig. 1 [13].

2.2. *Piezoelectric AFM*

Atomic force microscopes (AFM) are well known as a powerful tool for imaging pictures of atoms or observing surfaces on nanometer scale by scanning a fine

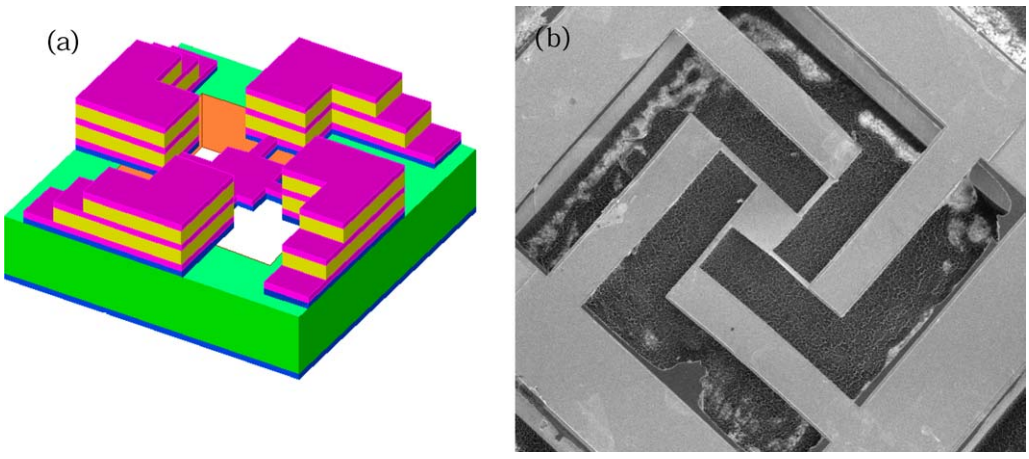

Fig. 1. Schematic draw of optical scanning device with double layered PZT layer (a) and the fabricated device, (b) Mirror plate: 300 × 300 (μm^2, DPZT beam: 800 × 230 μm^2).

ceramic or semiconductor tip over a surface. Typically, the tip is positioned at the end of a silicon-based cantilever beam. As the raster-scan drags the tip over the sample, the cantilever beam deflects. The magnitude of the deflection is captured by a laser that reflects at an oblique angle from the very end of the cantilever, and this indicates the local sample height. An AFM can work in contact mode, which measures the contact repulsive force with the tip touching the sample, or in noncontact/tapping mode, in which the tip can tap across the surface without tip destruction and adhesion problems. In order to increase the sensitivity of force gradients, an AFM cantilever requires a low spring constant which is achieved by scaling down the cantilever size or hollowing it out as a V-shaped structure. To achieve higher scan speed, an AFM is designed with high resonant frequency and integrated with a piezoelectric actuator. Moreover, piezoelectric detectors or piezoresistors are generally built into a silicon cantilever, which is called a self-sensitive probe, in order to improve the complexity of the data readout using an optical system.

The first AFM conceived by Binnig et al. in 1986 [14] stimulated the beginnings of an interest in developing the performance to implement AFM technology in industry such as by integrating it with semiconductor fabrication, refining scanning tip lithography techniques, use in high-density data storage devices and so on.

In 1989, Alexander et al. integrated an irradiation system and a position-sensitive photodetector as an optical lever system to greatly magnify the motion of the tip [15]. In noncontact AFM, the cantilever is vibrated near its resonant frequency and the tip is set at an extremely close distance from the sample. The vibration amplitude changes with the shift of the cantilever, which is modified by force gradients between the tip and the sample. This was used for measuring the vibration amplitude of the lever, and is called a heterodyne detector [16] or optical lever [17]. Due to the complexity of the alignment of the optical lever system, piezoelectric and piezoresistive ceramics were built into the cantilever to simplify the force-detecting system. In 1991, Tortonese et al. developed a piezoresistive cantilever as an integrated sensor by ion implantation and proved its efficient effects in the application of noncontact AFM [18]. Extending this first development, in 1995, Itoh and Suga proposed a single cantilever with two piezoelectric ZnO films for the inherent function of self-excited force sensing and z-axis actuation

Fig. 2. Fabricated AFM cantilever with XYZ actuation by PZT thin film layer.

[19, 20]. Minne et al. then integrated an actuator with ZnO film onto piezoresistive cantilever arrays, which is called parallel AFM [21–23]. This integrated piezoelectric actuator improved the scan speed of the AFM cantilever by eliminating the need for external z-axis actuation and greatly increased the resonant frequency corresponding to the imaging bandwidth. Moreover, since 1995, Fujii and Watanabe have been developing a lead zirconate titanate (PZT)-coated silicon cantilever which can perform either sensing displacement or actuation [24, 25]. Many researchers chose PZT over ZnO due to the higher piezoelectric constant and then improved the performance, for example, by integrating a PZT sensor and actuator in an AFM as illustrated in Figs. 2 [27] and 3 [28] or by eliminating electrical coupling problems at high frequency operation [26–29].

2.3. Hard Disk Drive Head

Hard disk drives with conventional single-stage servos cannot satisfy the requirements of precise positioning, high operating speed and frequency due to the development of ever-increasing track densities. A two-stage servo system consisting of a voice coil motor (VCM) and a microactuator was developed. In this two-stage servo scheme, the VCM would move the entire

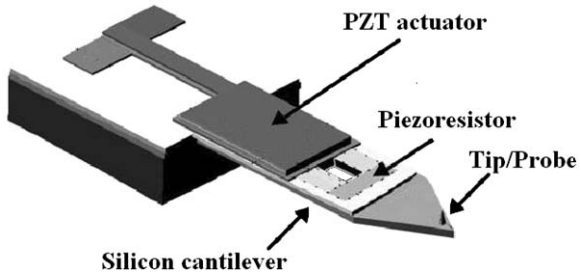

Fig. 3. Schematic drawing of self-actuation cantilever with an integrated piezoresistor.

head and arm at low frequency to perform coarse track seeking, and a microactuator would control the slider to perform high-frequency track following. Various microactuators, including piezoelectric, electromagnetic and electrostatic ones, have been developed. However, matching both requirements of necessary displacement stroke and high system resonant frequency is very difficult. In most cases so far, electrostatic and piezoelectric actuators have been applied in two-stage servo systems. Electrostatic actuators mainly using a comb drive scheme can perform linear or rotary actuations with precise positioning control. But the interdigitated finger structure has low stiffness springs, which decrease the resonant frequency of the total system. Additionally, to yield enough driving force, high voltage is necessary, which might possibly result in backlash and stiction problems. In case of piezoelectric actuators, piezoelectric ceramics with high stiffness can achieve high resonant frequency. With relatively lower driving voltage, a large force can be generated with very low power consumption. Their main disadvantage is the relatively low positioning accuracy compared with electrostatic actuators.

3. Membrane Type Actuator

3.1. What is a Membrane Type Actuator?

Until now, bulk piezoelectric actuators such as piezo-stacks or bimorph piezo-discs, have been used in many piezoelectric actuator applications because of the low actuation force and low displacement in thin film piezoelectric actuators. In the fabrication processes of bulk piezoelectric actuators, epoxy glue is used to bond to a bulk micromachined silicon membrane structure. These processes have many drawbacks in mass production. The use of a membrane (diaphragm) structure can solve the problem of low actuation force and low displacement in thin film piezoelectric actuators. This structures flexures is caused by end clamps. They naturally actuate with an 'S' shape because of increasing hysteresis due to creep in the bonds. This effect can further enhance the displacement and is attractive in piezoelectric applications such as ultrasonic fluid delivery and acoustic wave micromixers.

A membrane type actuator is usually composed of the released silicon structure as shown in Fig. 4. These structures can be patterned by an anisotropic chemical etching process using etchants like KOH, TMAH [30, 31], or a deep reactive ion etching process [32]. There are various membrane actuator types as shown in Fig. 4(a)–(c). The simple structure has applications in ultrasonic fluid drives and micromirrors, and can be fabricated by silicon anisotropic etching as shown in Fig. 4(a). For pumps, valves, and ink-jet print heads, the membrane type actuator shown in Fig. 4(b) is used with microfluidic channels fabricated with glass or a polymer like PDMS. The structure in Fig. 4(c) is compatible with surface micromachining technology using piezoelectric thin film actuators coated on sacrificial layers.

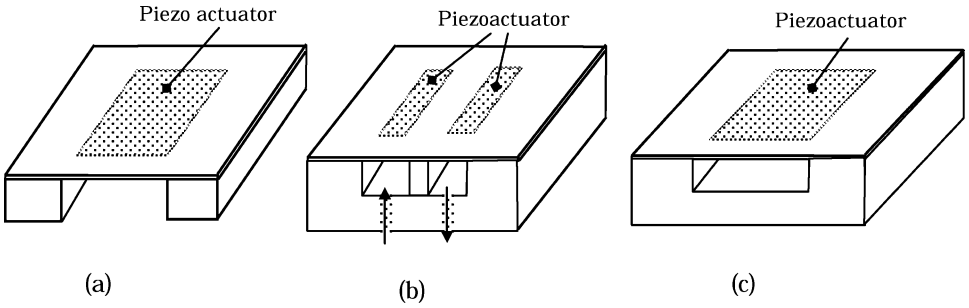

Fig. 4. Piezoelectric membrane actuator fabricated using micromachining technology.

This process is very simple and the fabricated structure is stable mechanically. For membrane type piezoelectric actuators, thin and thick piezoelectric films are coated on silicon membrane structures. There are several methods for coating the piezoelectric layer, such as the sol-gel process, sputtering techniques, chemical vapor deposition for thin piezoelectric film, screen printing methods, and spray coating. For these applications a rather thicker piezoelectric film is desired. However it is not easy to obtain films thicker than 1 mm by conventional deposition methods. Screen printing is now widely used for such applications, but the machining resolution is not yet satisfactory.

3.2. *Piezoelectric Actuator Applications Using Membrane Type*

Both thin films and thick films are used for the fabrication of piezoelectric membrane type actuators. Micropumps and valve devices, ink-jet print heads, ultrasonic fluid drives for microfluid applications are the targets of interest for industrial applications.

3.2.1. Piezoelectric actuated micro pump or valve in fluid applications. Microactuators for micropumps or valves are being increasingly applied in total analysis microsystems, labs on a chip, and chemical microreactors. Recently, micropumps driven by piezoelectric actuators have been studied for use in microfluid control systems. The displacement to pump the fluid can be easily controlled by applied voltage and the fabrication is simple. Conventionally bulk piezoelectric materials have been used as actuator materials. In spite of the low force output, piezoelectric thick film actuators are better for miniaturizing these devices than bulk type actuators.

A membrane type actuator using piezoelectric thick film for a micropump was reported by Koch et al. [33]. They utilized screen printing technology to form a thick piezoelectric film as shown in Fig. 5. The thick film was coated on a fusion bonded silicon membrane whose thickness was controlled by KOH etching. This method can yield higher output force and displacement in the piezoelectric membrane than the sol-gel or physical vapor deposition methods.

A micro-ink-jet application using a screen-printed PZT actuator was reported by a research group at SAIT, Korea [34]. For the piezoelectric actuation method, they used the bending mode for micropumping devices.

3.2.2. Piezoelectric actuator application using spray coating technology. Recently, various deposition methods for forming thick piezoelectric film such as aerosol deposition, spray coating, and ink-jet printing have been investigated by many researchers. The merits of these deposition methods over the screen-printing method are simplicity without etching and the capability of non-planar surface coating. These methods have been applied to a microparticle delivery system using acoustic waves, micropositioner for hard disk drive, ink-jet printer head, medical applications, and optical microlenses.

A research group has reported fabricating a PZT thick film by the aerosol deposition method (ADM) [35]. This method simplified the fabrication process by eliminating the etching process by using a stencil mask. A high deposition rate of 30 micron/min was attained in a 5 × 5 mm area at temperatures of less than 600

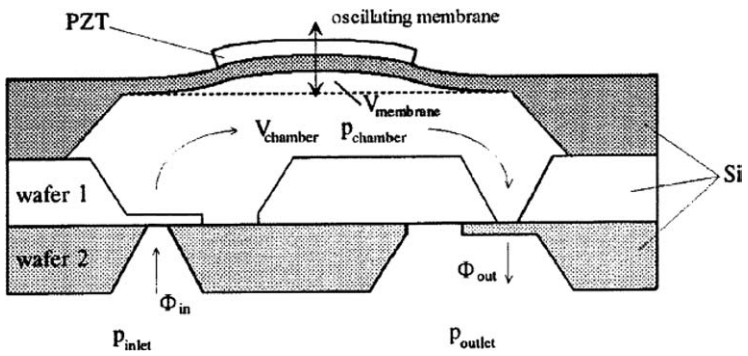

Fig. 5. Micropump using screen-printed PZT actuator on silicon membrane. (Courtesy of Neil White, Univ. of Southampton, UK.)

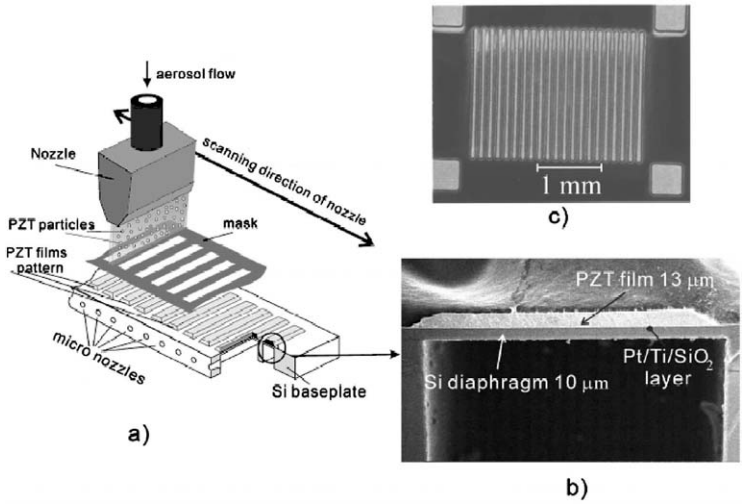

Fig. 6. (a) Schematic of aerosol deposition method: fabrication of micropump array, (b) Cross-sectional SEM image of 13-μm-thick Si diaphragm, and (c) Line patterning of PZT (optical image).

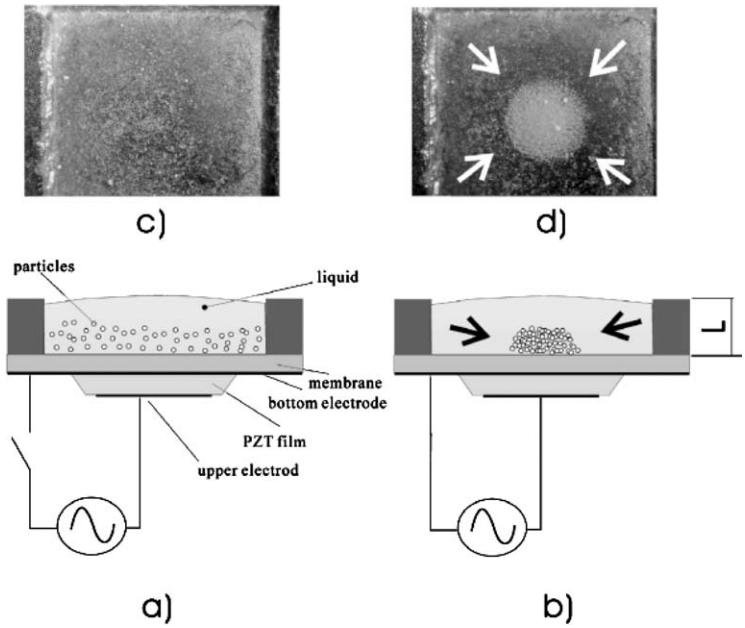

Fig. 7. Microparticle delivery system by aerosol deposition method (Courtesy of J. Akedo, AIST, Japan [14].)

degrees as shown in Fig. 6. To demonstrate applications of PZT thick film by the aerosol deposition method, the group fabricated microfluidic systems such as micropumps, microvalves, and microparticle delivery systems as illustrated in Fig. 7. They are also interested in fabricating micropositioning actuators for hard disk drives using this deposition method.

Spray coating has been developed at AIST, Japan [36] as shown in Fig. 8. The ejected fine liquid particles were carried by a jet stream of carrier gas onto the silicon substrate. The spray coating method has merits of capability of the dry and wet deposition conditions without damaging the substrate compared with the other thick film deposition methods.

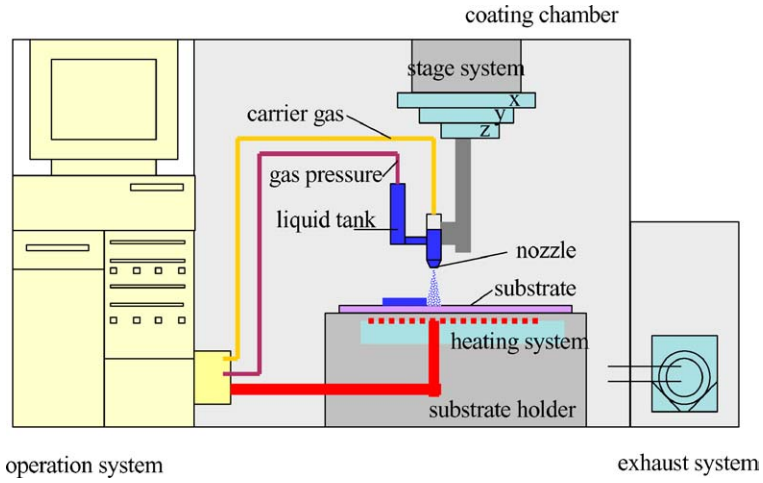

Fig. 8. Spray coating system equipment.

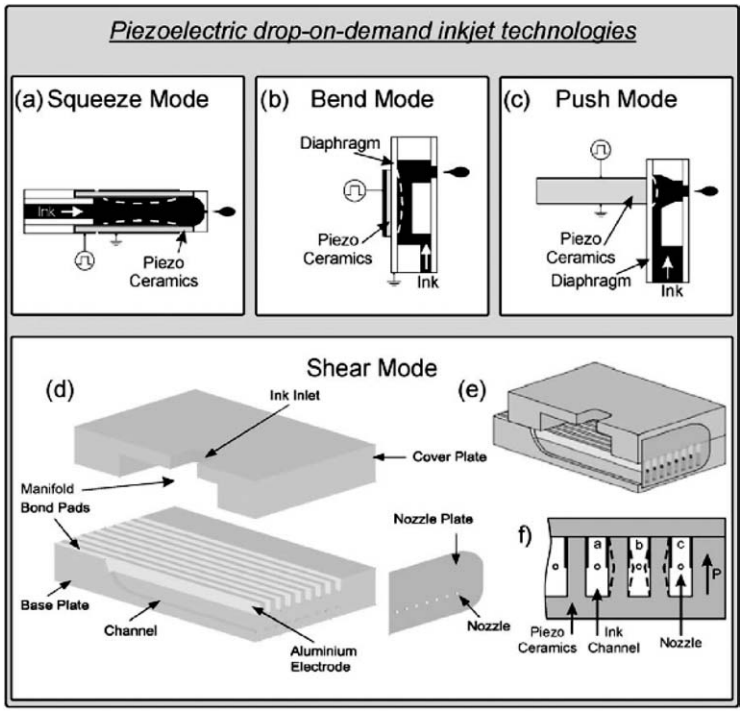

Fig. 9. Basic map of piezoelectric drop-on-demand inkjet technologies. (Courtesy of A.M. Grishin, Royal Institute of Technology, Sweden.)

A microactuator for ejecting the ink is necessary for an ink-jet print head system. A piezoelectric actuator for drop-on-demand ink-jet printing was reported by Grishin as shown in Fig. 9 [37]. Piezoelectric drop-on-demand technologies and micromachined droplet ejectors for controlled ink-jet printing can be utilized for piezoelectric thin or thick film formation by generating a transducer wave [38, 39].

Micro actuator for ejecting the ink is necessary for ink jet head system. Piezoelectric actuator for

drop-on-demand ink-jet was reported by Grishin as shown in Fig. 9 [37]. Piezoelectric drop-on-demand technologies and micromachined droplet ejector for controlled ink-jet printing can be utilized for piezoelectric thin or thick film formation by generating transducer wave [38, 39].

3.2.3. Ultrasonic applications. Thin film lamb waves or thin film flexural-plate wave actuators have advantages over bulk-plate wave actuators for transporting suspensions in fluids and fluid delivery applications [40]. For these applications, piezoelectric materials such as aluminum nitride, zinc oxide, and lead zirconate titanate have been utilized. Controlled membrane thickness less than the acoustic wavelength can be fabricated using the silicon backside etching process. For a piezoelectric thin film interdigitated transducer (IDT), the electrodes are easily fabricated by semiconductor processes. The Lamb wave is suitable for delivery or pumping of minute particles in fluids.

To overcome heat generation during mixing for temperature-sensitive fluidic applications (e.g., DNA chip), an acoustic wave micromixer was used with a piezoelectric thin film membrane actuator. The Fresnel Annular Sector Actuator (FASA) was based on an acoustic-wave transducer and generates strong acoustic waves. A parylene dome-shaped diaphragm using a piezoelectric ZnO thin film acoustic transducer has also been reported [41].

3.2.4. Other applications using piezoelectric membrane actuator. A micromirror for auto-focusing light using a piezoelectric thin film membrane actuator has been demonstrated by Goto et al. [42]. This device was composed of a $Pb(Zr_{0.54}Ti_{0.46})O_3$ piezoelectric diaphragm actuator deposited by radio frequency (RF) magnetron sputtering on a silicon diaphragm fabricated by KOH etching. Power generation applications have been reported [43] that use the inverting electric bias field in PZT to improve the displacement like meander-line actuators. P3 microheat engines based on thin film PZT membrane transducers have been researched by Richards [44]. These devices were composed of two main components, a heat engine with a heat source and a power generator with a piezoelectric transducer. The PZT-based MEMS power generator obtained several mW over 2 volts at frequencies between 300 and 1100 Hz.

3.3. Bulk Material Actuator and High Aspect Ratio Micro Structure

The advantages of bulk actuators, compared with cantilever and membrane thin film types, are the high performance of actuation and high reliability of piezoelectric characterization. Established manufacturing methods for bulk materials have better reliability than thin film methods. Bulk actuators have disadvantages in the mass production of MEMS substrates and in reliability because of the existence of the bonding glue layer. It is, therefore, necessary to form direct bonding between the bulk actuator layer and the device structure. In the following section, recent research trends of bulk actuators are introduced. High aspect ratio microstructures (HARMST), which do not fall in the cantilever, membrane or bulk actuator categories, are also introduced.

3.3.1. Bulk actuator. A parallel-bimorph-type piezoelectric actuator, which consists of two bimorphs arranged parallel to each other, for a high-resolution imager that uses CCD-chip-shift operations for practical applications has been developed [45]. From an investigation of the basic characteristics, it has been confirmed that the proposed actuator has achieved a sufficiently low voltage drive and high-speed response for the high-resolution imager using CCD-chip-shift operations. As a result, a box-shaped package of an imager, with a 22-pin, dual-in-line format, and dimensions of 30(L) $\times$ 20(W) $\times$ 11(H) mm was obtained as a usable size. A demand displacement of 8.5×10^{-3} mm was obtained at a driving voltage of 13 Vp-p (30 Hz pulses).

A valveless micropump based on a novel flow rectification principle using the temperature dependence of the liquid viscosity has been proposed [46]. A prototype device was fabricated by micromachining technology, as shown in Fig. 10. There is a linear relationship between the flow rate and pulse length of the heating signals. The contribution of local preheating of the liquid was not detected. These findings imply that a strong damping mode was realized. The maximum flow rate was limited by the decrease of the temperature difference and the generation of the vapor bubbles. The feasibility of this new pump principle has been confirmed, including the capability of bi-directional pumping.

An active micromixer for continuous flow has been proposed [47]. Mixing occurs directly by ultrasonic vibration. The patterns of inlets, outlets and mixing

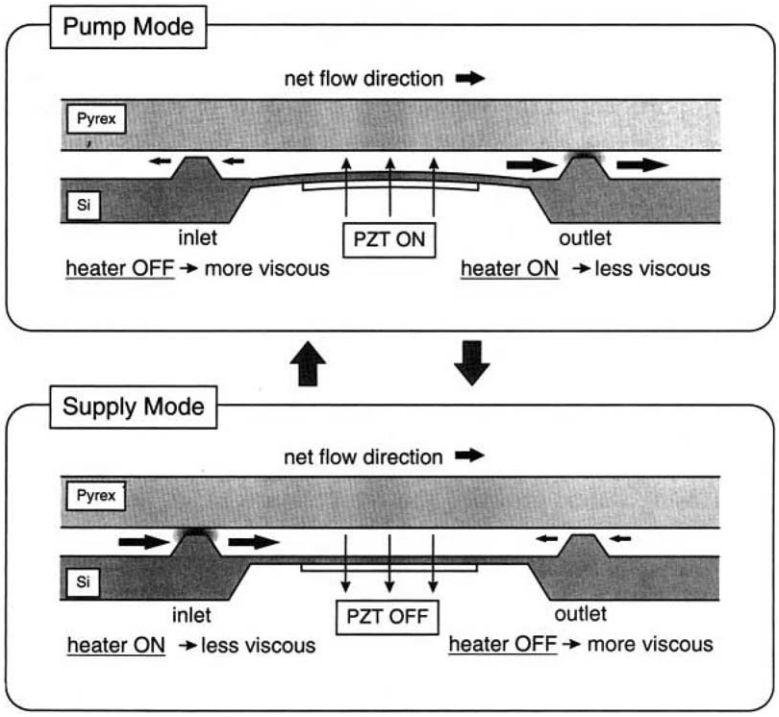

Fig. 10. Structure and operating sequence of a viscosity-based dynamic valve pump.

chamber were formed in glass. The entire flow path was encapsulated by anodic bonding of a Si wafer to the glass. A diaphragm ($6 \times 6 \times 0.15$ mm) was etched on the Si side to prevent ultrasonic radiation from escaping to the other parts of the device. The ultrasonic vibration originated from a bulk piezoelectric lead-zirconate-titanate (PZT) ceramic ($5 \times 4 \times 0.15$ mm). The PZT was adhered to the diaphragm and was excited by a 60 kHz square wave at 50 V (peak-to peak). Liquids were mixed in a chamber ($6 \times 6 \times 0.06$ mm) with the Si oscillating diaphragm driven by the PZT. A solution of uranine and water was used to evaluate the effectiveness of the mixing. The entire process was recorded using a fluorescent microscope equipped with a digital camera. The laminar flows of the uranine solution (5 ml/min) and water (5 ml/min) were mixed continuously and effectively when the PZT was excited. The temperature rise of the device was 15°C due to the ultrasonic irradiation.

The first-ever all-surface micromachined ultrasonic microrotor has been proposed [48]. The construction of the device is shown in Fig. 11. The rotor is actuated by electrically driving a piezoelectric PZT plate mounted at the back of a silicon die, eliminating the need for interconnects and space-consuming surface actuators. The rotor operates with single-phase sub-5V peak-to-peak excitation in atmospheric pressure. The piezoelectric plate is adhesively mounted making the method suitable for actuating micromachines from any surface micromachine process. Two different modes of operation have been demonstrated: pulsed and resonant. The pulse actuation results in a low rotation rate (0.5 to 3 RPM) while resonant actuation results in fast

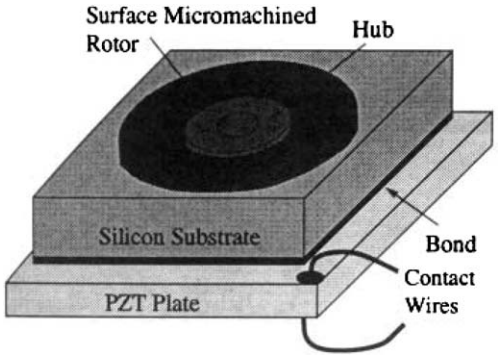

Fig. 11. Surface micromachined rotor actuated by a PZT plate.

rotation (10 to 100 RPM). The ability to drive a geared-down rotor (50:7), much smaller than the driving rotor, indicates high torque output capability.

The miniaturization of low power (typically 10 μW) and low rotation speed (about 100 rpm) motors for wristwatch applications has been proposed [49]. These motors are based on the conversion of the standing wave of the piezoelectric activated silicon stator membrane into rotation. This conversion is realized by a microfabricated rotor. To achieve the miniaturization of actuators, their construction requires simple-structured components and easy configuration. The new micromotor stably rotates at any posture, and the starting torque was measured to be about 2.6 μNm.

This new type of piezoelectric micromotor consists of components that structure function flexibly such as the Smart structure, which is different from conventional actuators. This research has achieved a micromotor for practical use in micromechanism fields [50].

A centimeter-sized robot for 5 DOF micromanipulation has been proposed [51]. Each leg ($1.5 \times 1.5 \times 4.0$ mm) can move independently and in three orthogonal directions. The main component in the robot is a six-legged monolithic piezoceramic unit suitable for large-scale production. The mechanical walking mechanism uses solid multilayer piezoactuators that make it possible to achieve both functionality and high precision.

Optical micromachines are easily miniaturized in fabrication sizes and are controllable by optical energy supplied wireless from a remote point. An optically driven moving machine that moves like a caterpillar using optoelectronic principles has been proposed [52]. It would consist of two parts, a body made of a spring and temperature sensitive ferrite and feet made of piezoelectric devices (PZT).

3.3.2. High aspect ratio structure. An array of lead zirconate titanate (PZT) rods whose cross section is 25 μm square has been fabricated using synchrotron radiation (SR) lithography, and the effects of the aspect ratio (height/width) of the PZT rods on 1–3 piezoelectric composite properties were studied [53]. The cross section is shown in Fig. 12. The aspect ratio was between 3 and 9. The mechanical quality factor and acoustic impedance were found to depend weakly on the aspect ratio.

A novel Silicon (Si) mold process has been proposed to fabricate stacked PZT/Si microactuators which consist of parallel plates of piezoelectric PZT intercalated by Si electrodes [54]. The batch-fabrication process is capable of creating a multi-layer PZT structure with plates as thin as 18 mm, meaning that an actuator driving voltage of as low as 18 V would be sufficient for operation.

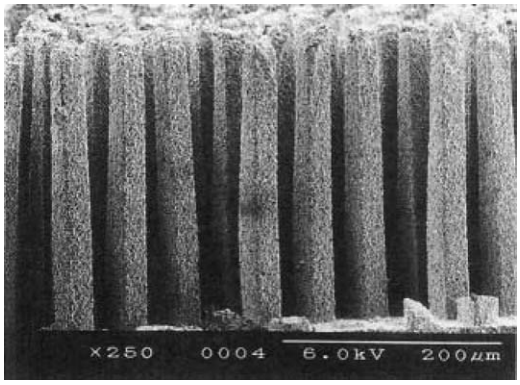

Fig. 12. PZT rod array (cross section: 25 μm).

3.3.3. Future problem. The direct bonding method has continued to be developed in recent years. Direct bonding between Si-wafer and Si-wafer, and between Si-wafer and single crystal have already been established [55]. This technology should become the key technology for mass production on bulk materials attached to MEMS. On the other hand, development of high-k ferroelectric single crystals has also been progressing recently [56]. The main application fields are limited to ultrasonic diagnosis at present. But some of these applications have the high performance of ferroelectrics and piezoelectric characteristics. Therefore these are promising for bulk actuator applications.

3.3.4. Summary of fabrication technologies. A comparison of fabrication technologies for piezoelectric actuators is given in Table 1.

The thickness of the film actuator is typically less than 1 mm. The film has a flat surface and is suitable for micromachining, e.g., photolithography, ion-milling, which could achieve a microactuator that is less than 1 mm thick. It is also easy to control the crystal orientation and to grow the crystal structure epitaxially in thin film. The improvement of material properties is, therefore, easier than with other technologies. On the other hand, it is also possible to form thick films from 1 to 50 mm in thickness. The firing temperature is

Table 1. Representative character of fabrication technologies for piezoelectric actuator.

	Thin film on Si	Thick film on Si	Bulk actuator on Si (Bonding)
Actuator thickness	Less than 1 μm	1 to 50 μm	50 μm to 1 mm
Process temperature	500 to 700°C	800 to 900°C	R.T. to 400°C
Crystallinity and orientation	Polycrystal, orientated or epitaxially grown crystal	Polycrystal, random orientation	Polycrystal, random orientation
Elecrical properties	Inferior to bulk	Inferior to bulk	Good
Process	PVD, CVD, sputtering, laser ablation	Screen printing, jet printing system	Solid-state reaction method
Compatibility with IC process	Good	Intermediate	Bad

relatively lower than bulk, but the film density and electrical properties are inferior to those of bulk. The flatness of surface is not good and not suitable for microfabrication. On the other hand, the output power of thick film is much better than that of thin film and is suitable for realizing relatively large-size devices. Therefore, if its problems are overcome, thick film is a good choice for microactuators. Bonding technology enables us to use the material properties of bulk directly. The actuator properties are, without a doubt, superior to those of other technologies. It is possible obtain the plate that thickness is less than 100 mm after the bonding process. On the other hand, microfabrication on bulk material has already been established. The bulk fabricated device size is over 100 mm and is larger than thin or thick film actuators. Room temperature bonding technology has been developed recently and could become a useful technology for MEMS applications.

4. Conclusion

Piezoelectric microactuators for MEMS were introduced classified by their shapes, i.e. cantilever, membrane and bulk types. Various applications were presented, but thicker films with high and reliable electrical properties have yet to be developed, and etching technology must be established for further successful applications. The alternative method of bonding bulk ceramics is being employed for fabrication, but the bonding technology is still under development.

References

1. P. Muralt, *J. Micromech. Microeng.*, **10**, 136 (2000).
2. E. Quandt and H. Holleck, *Microsystem Technologies*, **1**, 178 (1995).
3. D.L. Polla, *Proceedings of SPIE* (Austin, 1997), p. 24.
4. M. Okuyama, *Sensors Update*, **6**, 79 (2000).
5. D. Hauden, *Piezoelectric Materials: Advances in Science, Technology and Applications*, edited by C. Galassi (Kluwer Academic Publishers, Netherland, 2000), p. 335.
6. T. Ikeda, *Fundamentals of Piezoelectricity* (Oxford University Press, Oxford, 1990).
7. K. Uchino, *Piezoelectric Actuators and Ultrasonic Motors* (Kluwer Academic Publisher, 1997).
8. V.J. Fowler and J. Schlafer, *Proc. IEEE*, **54**, 1437 (1966).
9. L.F. Frank and J.K. Lee, U.S. Patent 3,981,566 (21 Sept. 1976).
10. H. Goto and K. Imanaka, *Proc. SPIE, Miniature and Micro-Optics/Fabrication and System Applications*, **V1544**, 272 (1991).
11. Y. Ohtuka, H. Nishikawa, T. Koumura, and T. Hattori, *Proc. IEEE MEMS*, 306 (1995).
12. A. Schroth, C. Lee, S. Matsumoto, and R. Maeda, *Sensors and Actuators*, **A73**, 144 (1999).
13. J. Tsaur, L. Zhang, R. Maeda, and S. Matsumoto, *Jpn. J. Appl. Phys.*, **V41**, 4321 (2002).
14. G. Binnig, C.F. Quate, and Ch. Gerber, *Phys. Rev. Lett.*, **56**, 930 (1986).
15. S. Alexander, L. Hellemans, O. Marti, J. Schneir, V. Elings, P.K. Hansma, M. Longmire, and J. Gurley, *J. Appl. Phys.*, **65**, 164 (1989).
16. Y. Martin, C.C. Williams, and H.K. Wickramasinghe, *J. Appl. Phys.*, **61**, 4723 (1987).
17. G. Meyer and N.M. Amer, *Appl. Phys. Lett.*, **53**, 2400 (1988).
18. M. Tortonese, H. Yamada, R.C. Barrett, and C.F. Quate, *Proc. 6th Int. Conf. Solid-State Sensors and Actuators, Tranducers*, 448 (1991).
19. T. Itoh and T. Suga, *Sensors and Actuators*, **A54**, 477 (1996).
20. T. Itoh, T. Ohashi, and T. Suga, *Proc. IEEE MEMS*, San Deigo, USA 451 (1996).
21. S.C. Minne, S.R. Manalis, and C.F. Quate, *Appl. Phys. Lett.*, **67**, 3918 (1995).
22. S.R. Manalis, S.C. Minne, and C.F. Quate, *Appl. Phys. Lett.*, **68**, 871 (1996).
23. S.C. Minne, G. Yaralioglu, S.R. Manalis, J.D. Adams, J. Zesch, A. Atalar, and C.F. Quate, *Appl. Phys. Lett.*, **72**, 2340 (1998).
24. T. Fujii, S. Watanabe, M. Suzuki, and T. Fujiu, *J. Vac. Sci. Technol. B*, **13**, 1119 (1995).
25. T. Fujii and S. Watanabe, *Appl. Phys. Lett.*, **68**, 467 (1996).
26. T. Itoh, T. Suga, and C. Lee, *Appl. Phys. Lett.*, **69**, 2036 (1996).
27. J. Chu, R. Maeda, T. Itoh, K. Kataoka, and T. Suga, *Jpn. J. Appl. Phys.*, **V38**, 7180 (1999).

28. Y. Kim, H. Nam, S. Cho, J. Hong, D. Kim, and J. Bu, *Sensors and Actuators*, **A103**, 122 (2003).
29. C. Lee, T. Itoh, and T. Suga, *Sensors and Actuators*, **A72**, 179 (1999).
30. D.B. Lee, *J. Appl. Phys.*, **40**, 4569 (1969).
31. H. Seidel, L. Csepregi, A. Heuberger, and H. Baumgärtel, *J. Electrochem. Soc.*, **137**(11), 3612 (1990).
32. A.A. Ayon, X. Zhang, and R. Khanna, *Solid-State Sensor and Actuator Workshop* (Hilton Head Island, South Carolina, June 4–8, 2000), p. 339.
33. M. Koch, N. Harris, R. Maas, A.G.R. Evans, N.M. White, and A. Brunnschweiler, *Measurement Science and Technology*, **8**, 49 (1997).
34. S.H. Lee, J. Chung, S. Lim, and C.S. Lee, *Proceedings of the 2001 International Conference on Robotics and Automation* (Seoul, Korea, May 21–26, 2001), p. 616.
35. J. Akodo and M. Lebedev, *Nano- and Micortechnology: Materials, Processes, Packaging, and System, SPIE*, vol. 4936 (2002), p. 234.
36. M. Ichiki, L. Zhang, Z. Yang, T. Ikehara, and R. Maeda, *Internal Conference Conference on Solid-State Sensors and Actuators* (2003), to be presented.
37. J. Brünahl and A.M. Grishin, *Sensors and Actuators*, A **101**, 371 (2002).
38. S. Okamura, R. Takeuchi, and T. Shiosaki, *Japanese Journal of Applied Physics*, **41**, 6714 (2002).
39. G. Percin and B.T. Khuri-Yakub, *Review of Scientific Instruments*, **73**(5), 2193 (2002).
40. P. Luginbuhl, S.D. Collins, G.-A. Racine, M.-A. Grétillat, N.F. de Rooij, K.G. Brooks, and N. Setter, *Journal of Microelectromechanical systems*, **6**(4), 337 (1997).
41. V. Vivek, Y. Zeng, and E.S. Kim, *The 13th Annual International Conference on Micro Electro Mechanical Systems* (2000) p. 668.
42. M. Sakata, S. Wakabayashi, H. Totani, M. Ikeda, H. Goto, M. Takeuchi, and T. Yada, *8th International Conference on Solid-State Sensors and Actuators, and Eurosensors 95*, p. 422.
43. W.P. Robbins, D.L. Polla, T. Tamagawa, D.E. Glumac, and W. Tjhen, *J. Micromech. Microeng.*, **1**, 247 (1991).
44. C. Xu, J. Hall, C. Richards, D. Bahr, and R. Richards, *ASME IMECE MEMS Symposium MEMS 2* (2000), p. 261.
45. C. Tanuma, *Jpn. J. Appl. Phys.*, **38**, 5603 (1999).
46. S. Matsumoto, R. Maeda, and A. Klein, *Micro. Thermo. Eng.* **3**, 31 (1999).
47. Z. Yang, S. Matsumoto, H. Goto, M. Matsumoto, and R. Maeda, *Sensors and Actuators*, **A93**, 266 (2001).
48. V. Kaajakari, S. Rodgers, and A. Lal, *Proc. IEEE MEMS*, 40 (2000).
49. L. Dellmann, S. Gautsch, G.A. Racine, and N.F. de Rooij, *Proc. Transducers'99*, 1752 (1999).
50. Y. Suzuki, K. Tani, and T. Sakuhara, *Proc. Transducers'99*, 1748 (1999).
51. U. Simu and S. Johnsson, *Proc. Transducers01*, 690 (2001).
52. K. Fukushima, Y. Otani, and T. Yoshizawa, *J. Pre. Mech. Eng.*, **64**, 1512 (1998).
53. Y. Hirata, T. Numazawa, and H. Takada, *Jpn. J. Appl. Phys.*, **36**, 6062 (1997).
54. S.N. Wang, K. Wakabayashi, J.F. Li, and M. Esashi, *Proc. of Transducers'99*, 1762 (1999).
55. H.Takagi, R. Maeda, N. Hosoda, and T. Suga, *Japanese Journal of Applied Physics*, Part 2, **38**, L1559 (1999).
56. Y. Hosono, K. Harada, T. Kobayashi, K. Itsumi, M. Izumi, Y. Yamashita, and N. Ichinose, *Jpn. J. Appl. Phys.*, **41**, 7084 (2002).